On the Thresholds of Generalized LDPC Convolutional Codes Based on Protographs

Lentmaier, Michael; Fettweis, Gerhard

Published in:
2010 IEEE International Symposium on Information Theory

DOI:
10.1109/ISIT.2010.5513595

2010

Proceedings 2010 International Symposium on Information Theory, to appear.

On the Thresholds of Generalized LDPC Convolutional Codes Based on Protographs

Michael Lentmaier and Gerhard P. Fettweis
Vodafone Chair Mobile Communications Systems
Dresden University of Technology (TU Dresden), 01062 Dresden, Germany
Emails: {michael.lentmaier, fettweis}@ifn.et.tu-dresden.de

***Abstract*—A threshold analysis of terminated generalized LDPC convolutional codes (GLDPC CCs) is presented for the binary erasure channel. Different ensembles of protograph-based GLDPC CCs are considered, including braided block codes (BBCs). It is shown that the terminated PG-GLDPC CCs have better thresholds than their block code counterparts. Surprisingly, our numerical analysis suggests that for large termination factors the belief propagation decoding thresholds of PG-GLDPC CCs coincide with the ML decoding thresholds of the corresponding PG-GLDPC block codes.**

I. Introduction

It can be observed that terminated protograph-based LDPC convolutional codes (PG-LDPC CCs) have better belief propagation (BP) decoding thresholds than their tailbiting versions or the block codes their are constructed from [1]. An analysis reveals that this can be prescribed to the slight irregularity at the ends of their Tanner graphs. This effect is visible even if the termination factor tends to infinity and both the code rate and degree distributions approach those of the corresponding block codes. A comparison with upper bounds on ML decoding thresholds presented in [2] shows that for infinite termination factors the BP thresholds $\varepsilon_{\infty,\mathrm{BP}}$ of regular LDPC CC ensembles must be close to the ML decoding thresholds of the regular block codes for both the binary erasure channel (BEC) and the additive white Gaussian noise (AWGN) channel. It can be observed, that on the BEC they actually numerically *coincide* with the tighter upper bounds $\varepsilon_{\mathrm{blk,ML}}$ on the ML thresholds presented in [3], which are based on BP EXIT functions [4] (see Table I). The same can also be verified for the convolutional code version of the irregular ARJA ensembles [5] investigated in [6]. More recently, for regular codes and the BEC, the equality of BP thresholds of convolutional ensembles and ML thresholds of the underlying block ensembles has been proven analytically in [7].

	$\varepsilon_{\mathrm{blk,BP}}$	$\varepsilon_{\infty,\mathrm{BP}}$	$\varepsilon_{\mathrm{blk,ML}}$
(3,6)	0.4294	0.4881	0.4881
(4,8)	0.3834	0.4977	0.4977
(5,10)	0.3416	0.4994	0.4994
ARJA	0.4387	0.4997	0.4997

TABLE I
THRESHOLDS OF SOME PG-LDPC ENSEMBLES.

In this paper, based on the transfer functions derived in [8], we extend the threshold analysis of PG-LDPC CCs [1] [6] [9] to generalized LDPC (GLDPC) codes. In addition to the recently investigated protograph-based braided block codes (PG-BBCs) [10] [11] we present some further PG-GLDPC ensembles and compare their thresholds with the upper bounds $\varepsilon_{\mathrm{blk,ML}}$. It turns out that $\varepsilon_{\infty,\mathrm{BP}}$ and $\varepsilon_{\mathrm{blk,ML}}$ are numerically equal for all investigated PG-GLDPC ensembles.

II. Thresholds of Protograph Ensembles

A. Protograph GLDPC Codes

A protograph is a bipartite graph consisting of a set of variable nodes V_n with degree J_n, $n = 1, \ldots, N_P$, a set of constraint nodes C_m with degree K_m, $m = 1, \ldots, M_P$ and a set of edges that connect them. The edges connected to a variable node V_n or a constraint node C_m are labeled by $e^{\mathrm{v}}_{n,j}$ or $e^{\mathrm{c}}_{m,k}$, respectively, where $j = 1, \ldots, J_n$ and $k = 1, \ldots, K_m$. The j-th edge of V_n is connected to the k-th node of C_m if $e^{\mathrm{v}}_{n,j} = e^{\mathrm{c}}_{m,k}$. In protograph-based GLDPC (PG-GLDPC) codes, each constraint node C_m can represent an arbitrary block code $\mathcal{C}_m$ of length K_m. As an example, Fig. 1 shows a rate $R = 1/6$ "Hamming-doped" protograph [12], created from an accumulate-repeat-accumulate (ARA) code. This ARA protograph was "doped" by associating a shortened (6,3) Hamming code to one of its check nodes.

A protograph can be represented by means of an $M_P \times N_P$ bi-adjacency matrix $\mathbf{B}$, which is called the *base matrix* of the protograph. The entry in row m and column n of $\mathbf{B}$ is equal to the number of edges that connect nodes C_m and V_n. The

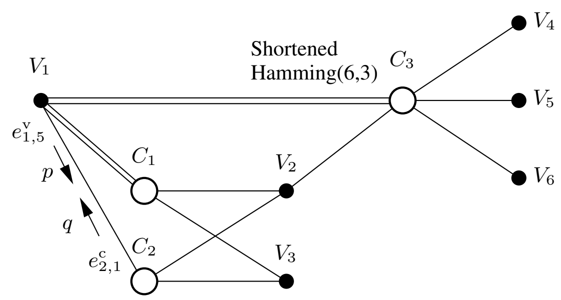

Fig. 1. Hamming-doped protograph with three constraint nodes C_m and six variable nodes V_n. Threshold: $\varepsilon^* = 0.8122$, Shannon limit: $\varepsilon_{\mathrm{Sh}} = 0.8333$.

base matrix of the protograph in Fig. 1 is given by

$$\mathbf{B} = \begin{bmatrix} 2 & 1 & 1 & 0 & 0 & 0 \\ 1 & 1 & 1 & 0 & 0 & 0 \\ 2 & 1 & 0 & 1 & 1 & 1 \end{bmatrix} \quad . \tag{1}$$

In order to construct ensembles of PG-GLDPC codes, a protograph can be interpreted as a template for the Tanner graph of a derived code, which can be obtained by a copy-and-permute operation [13]. The protograph is *lifted* by replicating each node T times and the edges are permuted among these replica in such a way that the structure of the original graph is preserved. As a consequence, a density evolution analysis for PG-GLDPC ensembles can be performed within the protograph. Equivalently, the Tanner graph of an GLDPC code can be represented by a bi-adjacency matrix that is derived from a protograph by replacing each 1 in $\mathbf{B}$ by a permutation matrix and each 0 by an all-zero matrix[1]. An ensemble of protograph based GLDPC (PG-GLDPC) codes of length $N = TN_P$ is defined by the set of matrices that can be derived from a given protograph by all possible combinations of size T permutation matrices.

Assume that belief propagation is used for decoding, with log-likelihood ratios (LLRs) acting as messages. In every iteration i, first all constraint nodes and then all variable nodes are updated. The messages computed at a constraint node C_m are then equal to

$$L_{\mathrm{c}}^{(i)}(e^{\mathrm{c}}_{m,k}) = \log \sum_{\mathbf{v}\in\mathcal{C}_k^{m,0}} \prod_{k'\neq k} \exp\left(L_{\mathrm{v}}^{(i-1)}(e^{\mathrm{c}}_{m,k'})(1/2 - v_{k'})\right)$$
$$- \log \sum_{\mathbf{v}\in\mathcal{C}_k^{m,1}} \prod_{k'\neq k} \exp\left(L_{\mathrm{v}}^{(i-1)}(e^{\mathrm{c}}_{m,k'})(1/2 - v_{k'})\right) \quad , \tag{2}$$

where $k, k' \in \{1, \ldots, K_m\}$. Here we have partitioned $\mathcal{C}_m$ into the sets $\mathcal{C}_k^{m,0}$ and $\mathcal{C}_k^{m,1}$, corresponding to codewords $\mathbf{v}$ for which $v_k = 0$ and $v_k = 1$, respectively. The message $L_{\mathrm{c}}^{(i)}(e^{\mathrm{c}}_{m,k})$ corresponds to the k-th extrinsic output generated by an optimal APP decoder for component code $\mathcal{C}_m$, which is applied to the incoming messages of node C_m. The incoming messages in the first iteration are initialized by the channel LLRs of the neighboring variable nodes, i.e., $L_{\mathrm{v}}^{(0)}(e_{m,k'}) = L_{\mathrm{ch}}(V_n)$, where V_n is the variable node connected to $e_{m,k'}$.

The messages computed at a variable node V_n are equal to

$$L_{\mathrm{v}}^{(i)}(e^{\mathrm{v}}_{n,j}) = L_{\mathrm{ch}}(V_n) + \sum_{j'\neq j} L_{\mathrm{c}}^{(i)}(e^{\mathrm{c}}_{n,j'}) \quad , \tag{3}$$

where $j, j' \in \{1, \ldots, J_n\}$.

B. Density Evolution for PG-GLDPC Codes

For transmission over a BEC the messages that are passed between the nodes represent either an erasure or the correct symbol values 0 or 1. In this case the BP decoder is particularly simple and exact density evolution can be described explicitly. Let $q^{(i)}(e^{\mathrm{c}}_{m,k})$ denote the probability that the check to variable node message which is sent along edge $e^{\mathrm{c}}_{m,k}$ in decoding iteration i is an erasure. Assuming a conventional LDPC code, where $\mathcal{C}_m$ is a single parity-check code, this is the case if at least one of the incoming messages from the other neighboring nodes is erased, i.e.,

$$q^{(i)}(e^{\mathrm{c}}_{m,k}) = 1 - \prod_{k'\neq k} \left(1 - p^{(i-1)}(e^{\mathrm{c}}_{m,k'})\right) \quad , \tag{4}$$

where $p^{(i-1)}(e^{\mathrm{c}}_{m,k'})$, $k, k' \in \{1, \ldots, K_m\}$, denote the probabilities that the incoming messages computed in the previous iteration are erasures. In case of an arbitrary block code $\mathcal{C}_m$, equation (4) can be replaced by the general expression

$$q^{(i)}(e^{\mathrm{c}}_{m,k}) = f_k^{\mathcal{C}_m}\left(p^{(i-1)}(e^{\mathrm{c}}_{m,k'}), k' \neq k\right) \quad , \tag{5}$$

where $f_k^{\mathcal{C}_m}$ is a multi-dimensional input/output transfer function that characterizes the APP decoder that computes the messages $L_{\mathrm{c}}^{(i)}(e^{\mathrm{c}}_{m,k})$ corresponding to (2). Note that, in general, $f_k^{\mathcal{C}_m}$ can be different for each $k \in \{1, \ldots, K_m\}$ so that the order of edges connected to node C_m can affect the performance of the ensemble. A method for computing explicit expressions for the APP decoder output distributions that can be used in (5) was presented in [8]. It is based on a Markov chain analysis of the decoder metrics in a trellis representation of the block code $\mathcal{C}_m$.

The variable to check node message sent along edge $e^{\mathrm{v}}_{n,j}$ is an erasure if all incoming messages from the channel and from the other neighboring check nodes are erasures. Thus we have

$$p^{(i)}(e^{\mathrm{v}}_{n,j}) = \varepsilon \prod_{j'\neq j} q^{(i)}(e^{\mathrm{v}}_{n,j'}) \quad , \tag{6}$$

where $j, j' \in \{1, \ldots, J_n\}$ and ε is the erasure probability of the BEC.

C. Upper-bounding ML Thresholds with BP EXIT Functions

The extrinsic probability $p_{\mathrm{BP,extr}}$ that a symbol associated with variable node V_n remains erased after BP decoding with I iterations can be expressed as

$$p_{\mathrm{BP,extr}}(V_n, \varepsilon) = \prod_j q^{(I)}(e^{\mathrm{v}}_{n,j}) \quad . \tag{7}$$

Note that here the product is over *all* incoming messages of V_n and the intrinsic channel erasure probability is omitted in the expression but implicitly involved in the calculation of $q^{(I)}(e^{\mathrm{v}}_{n,j})$. The BP EXIT function $h_{\mathrm{BP}}(\varepsilon)$ [4] is given by the average of $p_{\mathrm{BP,extr}}$ over all transmitted variable nodes[2].

Consider a (2,7) regular PG-GLDPC ensemble with Hamming component codes of length $N_{\mathrm{cc}} = 7$, as illustrated in Fig. 2. The BP EXIT function of this ensemble is shown in Fig. 3. The vertical line indicates the channel value at which the grey area below the curve is equal to the rate of the ensemble, which forms an upper bound $\varepsilon_{\mathrm{ML}}$ on the threshold of an optimal ML decoder. This follows from the area theorem [14] and the fact that $h_{\mathrm{BP}}(\varepsilon)$ can never be below

[1]The entries of multiple edges between a pair of nodes are replaced by the sum of permutation matrices

[2]Punctured nodes which are not transmitted are excluded.

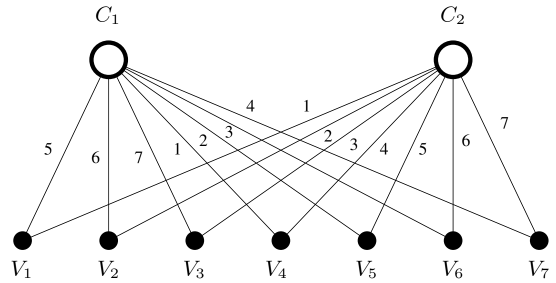

Fig. 2. Protograph of a (2,7) regular PG-GLDPC code. The edge labels denote the associated columns in the parity-check matrix of the component Hamming code.

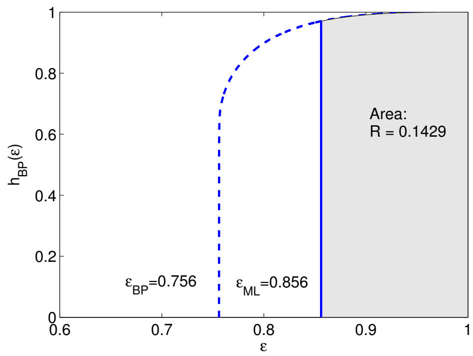

Fig. 3. BP EXIT function of a (2,7) regular PG-GLDPC code based on (7,4) Hamming component codes.

the EXIT function of the ML decoder. A detailed analysis of unstructured irregular ensembles, including results on the tightness of this bound, can be found in [4]. For structured protograph ensembles this technique has been applied in [3].

III. Terminated PG-GLDPC Convolutional Codes

Analogously to block codes, an ensemble of GLDPC convolutional codes can be constructed from a protograph. Such protograph-based GLDPC convolutional codes (PG-GLDPC CCs) can be described by means of a *convolutional protograph* [6] with base matrix

$$\mathbf{B}_{[-\infty,\infty]} = \begin{bmatrix} \ddots & & \ddots & & \\ \mathbf{B}_{m_{\mathrm{cc}}} & \dots & \mathbf{B}_0 & & \\ & \ddots & & \ddots & \\ & & \mathbf{B}_{m_{\mathrm{cc}}} & \dots & \mathbf{B}_0 \\ & & & \ddots & \ddots \end{bmatrix},$$

where m_{cc} denotes the memory of the convolutional codes and the $M_P \times N_P$ *component base matrices* $\mathbf{B}_i$, $i = 0, \dots, m_{\mathrm{cc}}$, describe the edges from the N_P variable nodes at time t to the M_P constraint nodes at time $t+i$. At time instant t the corresponding encoder creates a block $\mathbf{v}_t$ of TN_P symbols, resulting in the infinite code sequence $\mathbf{v} = [\dots, \mathbf{v}_1, \mathbf{v}_2, \dots, \mathbf{v}_t, \dots]$. The decoding constraint length is defined as $\nu = (m_{\mathrm{cc}}+1)TN_P$.

A. Protograph-Based Braided Block Codes

The protograph-based BBC (PG-BBC) ensembles considered in [11] are an example of PG-GLDPC CC ensembles as

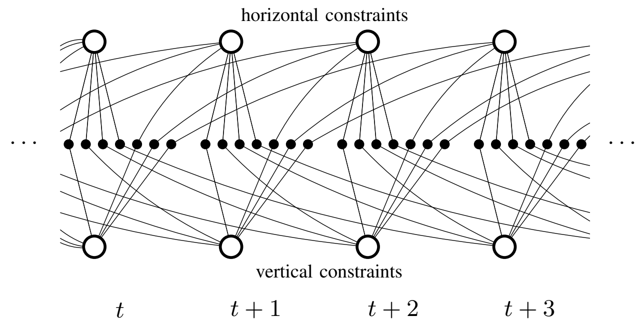

Fig. 4. Tanner graph of a PG-BBC with (7,4) Hamming component codes, defining Ensemble A_7. The nodes are grouped according to the time instant at which the code symbols are generated.

defined above. These can be derived by using the Tanner graph of a tightly BBC [10] as a protograph. The component base matrices of such a PG-BBC can be identified as

$$\mathbf{B}_0 = \begin{bmatrix} 1 & \mathbf{i} & \mathbf{0} \\ 1 & \mathbf{0} & \mathbf{i} \end{bmatrix}, \ \mathbf{B}_i = \begin{bmatrix} 0 & \mathbf{0} & \mathbf{e}_i \\ 0 & \mathbf{e}_i & \mathbf{0} \end{bmatrix}, \tag{8}$$

where $i = 1, \dots, m_{\mathrm{cc}}$, $\mathbf{e}_i = (0, \dots, 0, 1, 0, \dots, 0)$ is the length m_{cc} vector with a one at the i-th position and zeros elsewhere, $\mathbf{0}$ is the all-zero vector, and $\mathbf{i}$ the all-one vector. Throughout this paper we use the term Ensemble $A_{N_{\mathrm{cc}}}$ when referring to such PG-BBCs based on component codes of length N_{cc}.

For PG-BBCs with (7,4) Hamming component codes (i.e., $N_P = 7$ and $M_P = 2$), the resulting convolutional protograph is illustrated in Fig. 4. Its girth is equal to eight, which follows from the structure of the array and is true for any tightly BBC. Observe that the sum of the component base matrices is equal to the base matrix $\mathbf{B}$ of the corresponding GLDPC code, which is the all-one matrix of dimension $M_P \times N_P = 2 \times 7$. This reflects the fact that the graph of the PG-BBC in Fig. 4 can be obtained by repeating the GLDPC graph in Fig. 2 and permuting the edges among several adjacent time instants.

B. Convolutional Protographs with $m_{\mathrm{cc}} = 1$

Following the *edge-spreading* approach, considered in [6] for the design of PG-LDPC CCs, let us now consider some alternative constructions of PG-GLDPC CC ensembles. Starting from an arbitrary block protograph, defined by an $M_P \times N_P$ base matrix $\mathbf{B}$, we divide the edges among times $t, t+1, \dots, t+m_{\mathrm{cc}}$. For a given target memory m_{cc}, any set of component base matrices $\mathbf{B}_0, \mathbf{B}_1, \dots, \mathbf{B}_{m_{\mathrm{cc}}}$ which satisfies the condition

$$\sum_{i=0}^{m_{\mathrm{cc}}} \mathbf{B}_i = \mathbf{B} \tag{9}$$

corresponds to a possible assignment of edges, resulting in a convolutional protograph with the same variable and check node degrees as the original block protograph.

For the case $N_{\mathrm{cc}} = 7$, consider splitting $\mathbf{B}$ into component base matrices

$$\mathbf{B}_0 = \begin{bmatrix} 0 & 0 & 0 & 0 & 1 & 1 & 1 \\ 1 & 1 & 1 & 0 & 0 & 0 & 0 \end{bmatrix},$$

$$\mathbf{B}_1 = \begin{bmatrix} 1 & 1 & 1 & 1 & 0 & 0 & 0 \\ 0 & 0 & 0 & 1 & 1 & 1 & 1 \end{bmatrix},$$

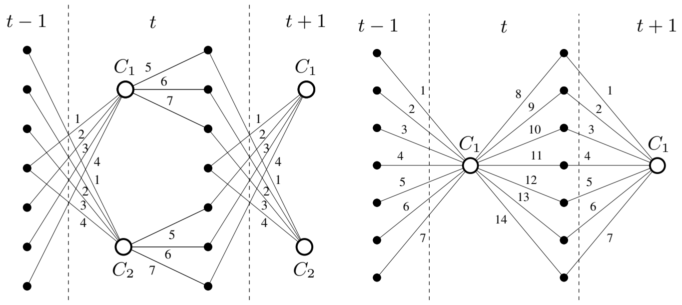

Fig. 5. Segments of the $m_{cc} = 1$ convolutional protographs defining Ensemble B_7 (left) and Ensemble C_{14} (right).

resulting in an ensemble of PG-GLDPC CCs with memory $m_{cc} = 1$, which we call Ensemble B_7. A segment of the corresponding convolutional protograph is shown in Fig. 5(left). A generalization to the Ensemble B_{15} and other values of N_{cc} is straightforward. While we can see that the reduced memory leads to a more compact representation of PG-GLDPC CCs, there is still some sparsity observable, reflected in a relatively low fraction of non-zero elements in the component base matrices $\mathbf{B}_0$ and $\mathbf{B}_1$. In case of even N_{cc} this can be eliminated by introducing multiple edges in the base matrix $\mathbf{B}$ of the block protograph. Considering shortened (14,10) Hamming codes as an example, we can use the nodes from the 2×7 protograph in Fig. 4 and connect each variable/check node pair with a double edge. We split the corresponding base matrix

$$\mathbf{B}_0 = \mathbf{B}_1 = \begin{bmatrix} 1 & 1 & 1 & 1 & 1 & 1 & 1 \end{bmatrix} , \qquad (10)$$

and obtain the protograph of Ensemble C_{14} with $M_P = 1$ check nodes and $N_P = 7$ variable nodes at each time instant, a segment of which is illustrated in Fig. 5(right). Since now $N_P = 7 = N_{cc}/2$, the ensemble has only half the constraint length as Ensemble B_{14} for a given lifting factor T. Puncturing the first variable node at each time instant t results in Ensemble $C_{14,P}$ with the asymptotic design rate $R_\infty = 0.5$.

C. Thresholds of Terminated PG-GLDPC CCs

Assume now that we start encoding at time $t = 1$ and terminate after L time instants. As a result we obtain a block protograph with the base matrix

$$\mathbf{B}_{[1,L]} = \begin{bmatrix} \mathbf{B}_0 & & \\ \vdots & \ddots & \\ \mathbf{B}_{m_{cc}} & & \mathbf{B}_0 \\ & \ddots & \vdots \\ & & \mathbf{B}_{m_{cc}} \end{bmatrix}_{M_P(L+m_{cc}) \times N_P L} . \qquad (11)$$

This terminated protograph is slightly irregular with lower constraint node degrees at the start and end. These shortened constraint nodes are now associated with shortened component codes in which the symbols of the missing edges are removed. Note that such a code shortening is equivalent to fixing these removed symbols and assigning an infinite reliability to them. The variable node degrees are not affected by termination.

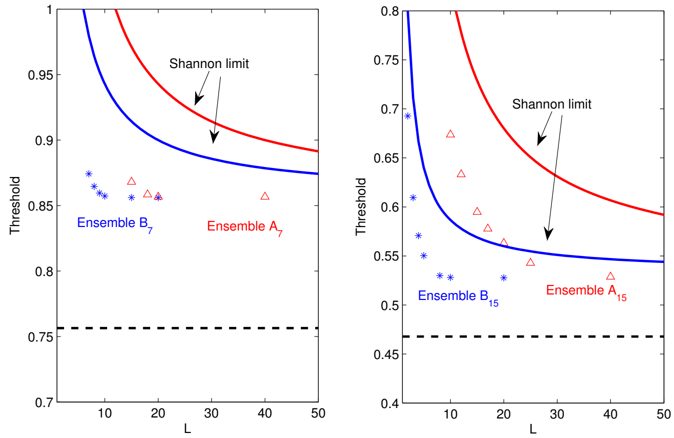

Fig. 6. BP decoding thresholds over termination factors L. Ensembles A_7 and A_{15} are shown in comparison with the ensembles B_7 and B_{15}, respectively. The dashed lines indicate the thresholds of the corresponding GLDPC block codes.

The parity-check matrix $\mathbf{H}$ of the block code, derived from $\mathbf{B}_{[1,L]}$ by lifting with some factor T, has $N = N_P L T$ columns and $M = M_P L M_{\mathcal{C}} T$ rows, were $M_{\mathcal{C}}$ denotes the number of parity-checks of the component code. It follows that the rate of the codes is equal to

$$R_L = 1 - \left(\frac{L + \Delta}{L} \right) \frac{M_P M_{\mathcal{C}}}{N_P} \qquad (12)$$

for some $\Delta > 0$ that accounts for the rate loss due to the termination. As $L \to \infty$, the rate R_L converges to the rate of the corresponding regular GLDPC code. Assuming full rank of $\mathbf{H}$, the rate loss coefficient can be identified as $\Delta = m_{cc}$. However, shortened component codes at the ends of the graph can cause a reduced rank of $\mathbf{H}$ that slightly increases R_L. In our examples, a rank loss could be observed for the PG-BBC Ensembles A_7 and A_{15}, based on Hamming component codes of length $N_P = 7$ and $N_P = 15$ (with $M_{\mathcal{C}} = 3$ and $M_{\mathcal{C}} = 4$, respectively), where the coefficients $\Delta = 2$ (instead of $m_{cc} = 3$) and $\Delta = 5.5$ (instead of $m_{cc} = 7$) could be observed by experiments with random liftings. No rank loss was observed for the considered ensembles with $m_{cc} = 1$.

The terminated PG-GLDPC CCs can be interpreted as PG-GLDPC block codes that inherit the structure of the convolutional codes. The length of these codes depends not only on the lifting factor T but also on the termination factor L. For a fixed L, the density evolution thresholds $\varepsilon_{L,\text{BP}}$ corresponding to codes with base matrix $\mathbf{B}_{[1,L]}$ can be estimated by recursive application of (6) and (5) for different channel parameters ε. The resulting thresholds for ensembles B_7 and B_{15} are compared in Fig. 6 with the BBC ensembles A_7 and A_{15} for different termination factors L. The thresholds of all the considered ensembles versus the code rate are shown in Fig. 7. Analogously to PG-LDPC CCs (see Table I), we observe that as $L \to \infty$ the BP thresholds numerically coincide with the upper bounds on the ML decoding thresholds of the corresponding block code ensembles. From the achievability of $\varepsilon_{\infty,\text{BP}}$ it follows that the bounds $\varepsilon_{\text{blk,ML}}$ are tight.

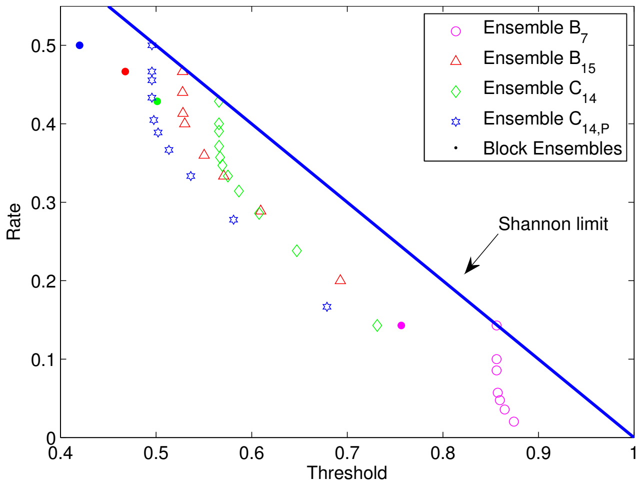

Fig. 7. BP decoding thresholds versus code rate for different PG-GLDPC convolutional code ensembles and termination factors.

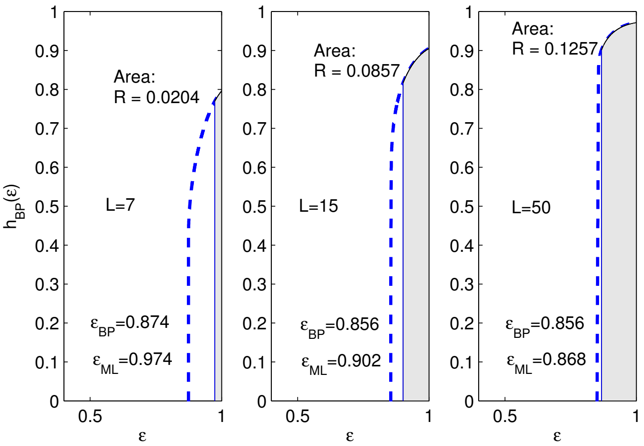

Fig. 8. BP EXIT functions of terminated PG-GLDPC convolutional codes from the ensemble B_7 for different termination factors L.

The BP EXIT functions of the terminated codes from ensemble B_7 are shown in Fig. 8. Indeed, with increasing L their BP thresholds converge to their ML thresholds, indicating optimality of BP decoding. Large L can be realistic in conjunction with window based decoders, like suggested in [15], where decoding delay and storage requirement depends on the window size W, where $W < L$, but is totally independent of the length L of the transmitted code sequences. For shorter L, which introduces a significant rate loss, the BP decoding of the terminated codes is clearly suboptimal but still provides a flexible adjustment of coding rate and threshold.

Acknowledgment

The authors would like to thank Dr. Gianluigi Liva for pointing out the numerical equality of the ML thresholds of regular block codes and the BP thresholds of asymptotically regular convolutional codes. The authors are also grateful for the use of the high performance computing facilities of the ZIH at TU Dresden.

References

[1] A. Sridharan, M. Lentmaier, D. J. Costello, Jr., and K. Sh. Zigangirov, "Convergence analysis of a class of LDPC convolutional codes for the erasure channel," in *Proceedings of the 42nd Allerton Conference on Communication, Control, and Computing*, Monticello, IL, USA, 2004.

[2] M. Lentmaier, A. Sridharan, D.J. Costello, Jr., and K.Sh. Zigangirov, "Iterative decoding threshold analysis for LDPC convolutional codes," *IEEE Trans. Inform. Theory*, accepted for publication. See also http://www.vodafone-chair.com/staff/lentmaier/LDPCCCThresholds_TransIT.pdf.

[3] E. Paolini, M. Varrella, M. Chiani, B. Matuz, and G. Liva, "Low-complexity LDPC codes with near-optimum performance over the BEC," in *Proc. 4th Advanced Satellite Mobile Systems. ASMS 2008.*, Aug. 2008, pp. 274–282.

[4] C. Measson, A. Montanari, and R. Urbanke, "Maxwell construction: The hidden bridge between iterative and maximum a posteriori decoding," *IEEE Trans. Inform. Theory*, vol. 54, no. 12, pp. 5277–5307, Dec. 2008.

[5] D. Divsalar, S. Dolinar, and C. Jones, "Construction of protograph LDPC codes with linear minimum distance," in *Proc. IEEE International Symposium on Information Theory*, Seattle, WA, July 2006, pp. 664–668.

[6] M. Lentmaier, G.P. Fettweis, K.Sh. Zigangirov, and D.J. Costello, Jr., "Approaching capacity with asymptotically regular LDPC codes," in *Proc. Information Theory and Applications Workshop*, San Diego, CA, Feb. 2009.

[7] Shrinivas Kudekar, Tom Richardson, and Rüdiger L. Urbanke, "Threshold saturation via spatial coupling: Why convolutional LDPC ensembles perform so well over the BEC," available online at http://arxiv.org/abs/1001.1826.

[8] M. Lentmaier, M.B.S. Tavares, and G.P. Fettweis, "Exact erasure channel density evolution for protograph based generalized LDPC codes," in *Proc. IEEE International Symposium on Information Theory*, Seoul, Korea, July. 2009, pp. 566–570.

[9] M. Lentmaier, A. Sridharan, K. Sh. Zigangirov, and D. J. Costello, Jr., "Terminated LDPC convolutional codes with thresholds close to capacity," in *Proc. IEEE International Symposium on Information Theory*, Adelaide, Australia, Sept. 2005, pp. 1372–1376.

[10] A.J. Feltström, D. Truhachev, M. Lentmaier, and K.Sh. Zigangirov, "Braided block codes," *IEEE Trans. Inform. Theory*, vol. 55, no. 6, pp. 2640–2658, June 2009.

[11] M. Lentmaier, B. Noethen, and G.P. Fettweis, "Density evolution analysis of protograph-based braided block codes on the erasure channel," in *Proc. 8th International ITG Conference on Source and Channel Coding*, Siegen, Germany, Feb. 2010.

[12] G. Liva, W.E. Ryan, and M. Chiani, "Quasi-cyclic generalized LDPC codes with low error floors," *IEEE Trans. Commun.*, vol. 56, no. 1, pp. 49–57, January 2008.

[13] J. Thorpe, "Low-density parity-check (LDPC) codes constructed from protographs," in *IPN Progress Report 42-154, JPL*, Aug. 2003.

[14] A. Ashikhmin, G. Kramer, and S. ten Brink, "Extrinsic information transfer functions: model and erasure channel properties," *IEEE Trans. Inform. Theory*, vol. 50, no. 11, pp. 2657–2673, Nov. 2004.

[15] M. Papaleo, A. Iyengar, P. Siegel, J. Wolf, and G. Corazza, "Windowed erasure decoding of LDPC convolutional codes," in *Proc. 2010 IEEE Information Theory Workshop*, Cairo, Egypt, Jan. 2010.